JACS
JOURNAL OF THE AMERICAN CHEMICAL SOCIETY
Article
pubs.acs.org/JACS

New Forms of CdSe: Molecular Wires, Gels, and Ordered Mesoporous Assemblies

Margaret H. Hudson,[†] Dmitriy S. Dolzhnikov,[†] Alexander S. Filatov,[†] Eric M. Janke,[†] Jaeyoung Jang,[†,∥] Byeongdu Lee,[‡] Chengjun Sun,[‡] and Dmitri V. Talapin*[,†,§]

[†]Department of Chemistry and James Franck Institute, The University of Chicago, Chicago, Illinois 60637, United States
[‡]Advanced Photon Source, Argonne National Laboratory, Argonne, Illinois 60439, United States
[§]Center for Nanoscale Materials, Argonne National Laboratory, Argonne, Illinois 60439, United States

Supporting Information

ABSTRACT: This work investigates the structure and properties of soluble chalcogenidocadmates, a molecular form of cadmium chalcogenides with unprecedented one-dimensional bonding motifs. The single crystal X-ray structure reveals that sodium selenocadmate consists of infinite one-dimensional wires of $(Cd_2Se_3)_n^{2n-}$ charge balanced by Na^+ and stabilized by coordinating solvent molecules. Exchanging the sodium cation with tetraethylammonium or didodecyldimethylammonium expands the versatility of selenocadmate by improving its solubility in a variety of polar and nonpolar solvents without changing the anion structure and properties. The introduction of a micelle-forming cationic surfactant allows for the templating of selenocadmate, or the analogous telluride species, to create ordered organic−inorganic hybrid CdSe or CdTe mesostructures. Finally, the interaction of selenocadmate "wires" with Cd^{2+} ions creates an unprecedented gel-like form of stoichiometric CdSe. We also demonstrate that these low-dimensional CdSe species show characteristic semiconductor behavior, and can be used in photodetectors and field-effect transistors.

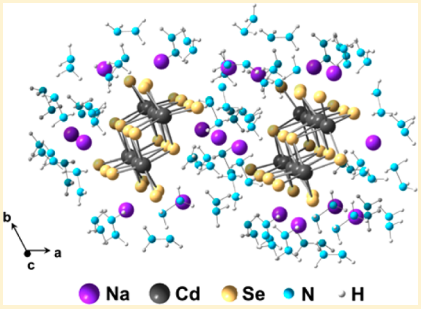

1. INTRODUCTION

Semiconductors play many important roles in modern information- and energy-related technologies. The ability of semiconducting materials to manipulate electrical charges and absorb or emit photons is utilized in electronic circuits, solar cells, light-emitting diodes, and many other devices.[1] II−VI semiconductors, the materials combining Zn, Cd, or Hg with chalcogens (O, S, Se, or Te), represent one of the most important semiconductor families and are widely utilized in solar cells,[2,3] photocatalysts,[4,5] IR detectors,[6,7] and other technologies. In recent years, significant progress has been achieved in the development of low-dimensional II−VI semiconductors in the form of quantum dots,[8,9] quantum rods,[10−12] and quantum wells (nanoplatelets)[13,14] that exhibit excellent light emission properties and are commercially used for biotags and display technologies.[15,16] Among low-dimensional semiconductors, CdSe has emerged as the most studied material and has been used as a model system in many optical[17,18] and electronic studies[19,20] of low-dimensional semiconductors. In this work we report three new forms of low-dimensional CdSe: molecular polymers, gels, and mesoporous assemblies.

The solution synthesis of low-dimensional materials typically involves chemical transformations of molecular species into a crystalline lattice through nucleation and growth steps. Currently, we do not have a good understanding of the mechanism of such transformations, and the structures of intermediate species remain to be revealed. Various solvothermal methods with metal salts and elemental chalcogens have been used to create species with one-, two-, and three-dimensional metal chalcogenide bonding frameworks with interesting morphologies and properties.[21−27] These approaches typically build up segments of metal chalcogenide lattice from molecular precursors. Interestingly, low-dimensional metal chalcogenides can also be accessed through disassembly of the bulk crystalline lattice. For example, Mitzi and co-workers utilized the reducing power of hydrazine to dissolve bulk metal chalcogenides in an excess of chalcogen at room temperature to generate soluble chalcogenidometallates.[28−35] Mitzi's approach produced chalcogenidometallates of Sn (S, Se, Te), Cu (S, Se), Ge (S, Se), In (Se, Te), and Zn (Te), but soluble products for many technologically important metal chalcogenides could not be obtained with this approach. We recently reported the synthesis of soluble chalcogenidometallate species for Cd, Pb, and Bi chalcogenides by combining strongly reducing chalcogenide salts (Na_2Ch, K_2Ch) with bulk metal chalcogenide in hydrazine.[36] These complexes were explored for their utility as "solders" for II−VI semiconductors. For example, a solution of the chalcogenidometallate could be mixed with ball-milled semiconductor powder and heated to 300 °C to form a polycrystalline film

Received: September 25, 2016
Published: February 1, 2017

DOI: 10.1021/jacs.6b10077
J. Am. Chem. Soc. 2017, 139, 3368−3377

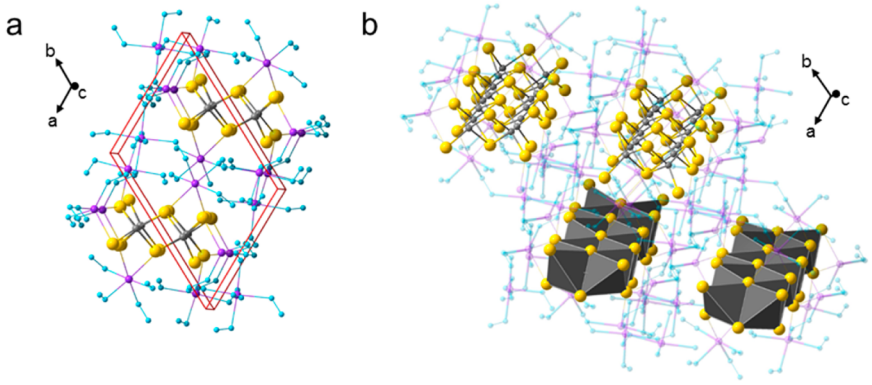

Figure 1. Single crystal structure for $Na_4Cd_4Se_6{\cdot}9.5N_2H_4$, where gray spheres represent Cd, yellow is Se, purple is Na, and blue is N: (a) viewed down the *c*-axis with hydrogen atoms omitted for clarity with unit cell outlined in red ($P\bar{1}$, a = 10.5623(10) Å, b = 13.5662(12) Å, c = 13.6038(11) Å, α = 104.728(3)°, β = 108.183(3)°, γ = 111.179(3)°, Z = 2); (b) a view highlighting Cd and Se chalcogenidometallate framework to demonstrate its wire-like morphology.

with good mechanical stability and electrical properties. These chalcogenidometallates also showed remarkable success as inorganic capping ligands for quantum dots; nanocrystals could be capped with composition-matched ligands and annealed at 300 °C to form polycrystalline metal chalcogenide films. Electron mobilities above 300 $cm^2\ V^{-1}\ s^{-1}$ were obtained for annealed films of CdSe nanocrystals capped with sodium selenocadmate, achieving half the mobility of single crystalline CdSe and far surpassing previously obtained mobilities for solution-processed films.[36,37]

In this study we report the structure of a polymeric form of $[Cd_2Se_3]_n^{2n-}$ which represents, to the best of our knowledge, the first molecular motif with a one-dimensional CdSe bonding framework. The negative charge of the $[Cd_2Se_3]_n^{2n-}$ chain can be counterbalanced with various inorganic or organic cations. The choice of cation can be used to tune the solubility of $[Cd_2Se_3]_n^{2n-}$ wires in polar and nonpolar solvents or to form a micellar template[38−42] to generate mesostructured CdSe. We also show that these molecular "wires" can be cross-linked with Cd^{2+} ions to create yet another new form of CdSe, a stoichiometric Cd−Se gel. This chemistry can be, at least partially, transferred to other II−VI semiconductors and brings new opportunities for solution-based processing of technologically important semiconductors.

2. EXPERIMENTAL SECTION

All manipulations were performed in a nitrogen glovebox with <10 ppm oxygen and water levels, unless otherwise noted. Further experimental details are given in the Supporting Information.

2.1. Synthesis of $Na_2Cd_2Se_3$. A 0.25 mmol portion of Na_2Se[43] was combined with 96 mg (0.5 mmol) of CdSe powder in 10 mL of hydrazine. This mixture was stirred at room temperature until it was colorless and the dark solid dissolved, about 5 days. The solution was filtered through a 0.45 μm PTFE syringe filter to remove any unreacted solids. The product was isolated by adding acetonitrile as nonsolvent and centrifuging to isolate a white solid. The solid was dissolved in hydrazine at concentrations up to ∼0.05 M.

2.2. Growth of $Na_4Cd_4Se_6{\cdot}9.5N_2H_4$ Crystals. Single crystals of $Na_2Cd_2Se_3$ were grown by slow evaporation of the hydrazine solvent. A solution of ∼0.025 M $Na_2Cd_2Se_3$ in hydrazine was loaded into a clean, dry glass tube in the glovebox. The tube had a 100° bend in the midsection, and the solution was loaded to fill one side of the bend halfway (∼0.5 mL). The tube was temporarily sealed under nitrogen, removed from the glovebox, and flame-sealed under mild vacuum. The side of the tube containing the solution was suspended over a warm hot plate (80 °C), and the other side was at room temperature. Over the course of about 2 weeks, the hydrazine evaporated from the warm side and collected in the cool side, leaving behind plate-like crystals.

2.3. NEt_4^+ Cation Exchange. To create $(NEt_4)_2Cd_2Se_3$, Amberlyst 15 highly acidic cation exchange resin was loaded with the desired cation and mixed in 10× excess with $Na_2Cd_2Se_3$. A 1 mg portion of resin was rinsed with 3 mL of ∼1.5 M $(NEt_4)OH$ in methanol 3 times and then dried under vacuum at 60 °C for an hour. After cation exchange, any excess resin was removed by filtering the solution through a 0.45 μm PTFE syringe filter.

2.4. Using $Na_2Cd_2Se_3$ as Ligands for Colloidal CdSe Nanocrystals. CdSe nanocrystals were synthesized using a literature procedure.[18,44] For ligand-exchange experiments, nanocrystals were washed an additional 5 times with methanol and 4 times with ethanol in a nitrogen glovebox. Ligand exchange from ODPA to $Na_2Cd_2Se_3$ or $(NEt_4)_2Cd_2Se_3$ was performed with slight modifications to a literature procedure.[36] A 1.4 mL portion of a solution of ODPA-capped CdSe nanocrystals (∼4 mg/mL) was layered atop 1.4 mL of a $Na_2Cd_2Se_3$ solution in hydrazine (∼7 mM). The solution was briefly vortexed, and the nanocrystals transferred to the hydrazine layer. The toluene-rich phase was removed, and the hydrazine-rich phase was washed 3 times with 1.4 mL of fresh toluene. Then, the nanocrystal solution in hydrazine was filtered through a 0.2 μm PTFE syringe filter. This solution was then precipitated with the addition of acetonitrile nonsolvent (∼1:1 hydrazine/acetonitrile), and the nanocrystals were redispersed in hydrazine. The above procedure was repeated for $(NEt_4)_2Cd_2Se_3$-capped CdSe, but the final step required more nonsolvent to precipitate the nanocrystals.

2.5. Preparation of Mesostructured CdSe. *N*-Eicosane-*N*,*N*-dihydroxyethyl-*N*-methylammonium bromide (EDHEMAB) was synthesized according to a literature procedure, where 1-bromoeicosane (7.22 g, 20 mmol) and *N*-methyldiethanolamine (2.29 mL, 20 mmol) were refluxed in EtOH for 24 h,[45] and the resulting white solid was washed with cold EtOH and recrystallized from 1:1 $CHCl_3$/EtOAc. EDHEMAB was dried under dynamic vacuum overnight and transferred into the glovebox. A 1 g portion of EDHEMAB was dissolved in 12 mL of N_2H_4 at 80 °C to form a clear, colorless solution, and 10 mL of 0.025 M $Na_2Cd_2Se_3$ was added dropwise, turning the solution cloudy white. This mixture was stirred at 40 °C for 3 h. A white solid was isolated by centrifugation, and washing with excess ethanol and hexane yielded a yellow powder. This yellow powder could be suspended in 1:1 hexane/ethanol and drop-cast for XRD or TEM analysis.

2.6. Synthesis of Na_2CdTe_2. A 2 mmol portion of Na_2Te was added to 480 mg of CdTe powder (2 mmol) in 4 mL of hydrazine. After approximately 2 days of stirring, all of the solid dissolved, leaving the solution clear yellow. The solution was filtered with a 0.2 μm PTFE syringe filter, and the solid was isolated through precipitation with acetonitrile nonsolvent and centrifugation. The solid Na_2CdTe_2

DOI: 10.1021/jacs.6b10077
J. Am. Chem. Soc. 2017, 139, 3368−3377

could be dissolved in hydrazine or formamide up to concentrations of ~0.5 M.

2.7. Preparation of Mesostructured CdTe. A 100 mg portion of EDHEMAB was dissolved in 2 mL of formamide at 80 °C. A 500 μL portion of a 0.1 M solution of Na_2CdTe_2 in hydrazine was added dropwise at 80 °C, and a yellow-orange precipitate formed immediately, suspended in a green solution. The temperature was decreased to room temperature, and the suspension was stirred for an hour. The solid was isolated by centrifugation and washed with excess NMF, ethanol, and hexane to yield a red-orange powder.

2.8. Preparation of Gel-like CdSe. A 50 μL portion of 0.5 M $CdCl_2$ in N_2H_4 was added to 1 mL of ~0.025 M $Na_2Cd_2Se_3$ in N_2H_4 and briefly vortexed to form a cloudy white suspension. After centrifugation for 10 s, a white or pale yellow gel-like material was collected, and the supernatant was discarded to remove excess reactant and NaCl. The gel can be resuspended in varying amounts of hydrazine to tune its viscosity. To form films, suspensions of the gel were drop-cast on piranha-treated glass or silicon substrates, dried at room temperature, and annealed at various temperatures for 30 min on a hot plate.

3. RESULTS AND DISCUSSION

3.1. $Na_2Cd_2Se_3$ Synthesis and Structural Characterization. Bulk CdSe powder completely dissolves in liquid hydrazine at room temperature in the presence of 0.5 molar equivalents of Na_2Se. After several days of stirring, the solution becomes colorless, and the chalcogenidometallate product can be isolated by addition of acetonitrile followed by centrifugation to yield a white powder. Inductively coupled plasma optical emission spectroscopy (ICP-OES) indicates that the product has the empirical formula $Na_2Cd_2Se_3$. This sodium selenocadmate is soluble up to ~0.05 M (25 mg/mL) in hydrazine.

To characterize this new chalcogenidometallate compound, colorless, platelike crystals were grown by slow evaporation of hydrazine from a ~0.025 M $Na_2Cd_2Se_3$ solution over the course of 2 weeks, and the structure was revealed by single crystal X-ray diffraction. The diffraction results show that this complex crystallizes in the $P\bar{1}$ space group with an asymmetric unit of $Na_4Cd_4Se_6{\cdot}9.5N_2H_4$ (Figure 1 and Figure S1). The selenocadmate anionic framework has a one-dimensional structure of double chains of distorted edge-sharing $[CdSe_4]$ tetrahedra running along the *c*-axis. The structure contains bridging Se^{2-} anions coordinated by four Cd^{2+} cations with bond distances ranging from 2.7210(7) to 2.7981(7) Å and terminal Se^{2-} anions bound to two Cd^{2+} cations through shorter bonds from 2.6075(7) to 2.6280(7) Å. These $(Cd_2Se_3)_n^{2n-}$ chains are charge balanced by Na^+ cations. The Na^+ either bridges two Se^{2-} or is bound to a single Se^{2-} with average Na–Se bond lengths of ~3 Å; the coordination sphere around Na^+ is filled with hydrazine in either an octahedral or trigonal bipyramidal configuration. Adjacent $(Cd_2Se_3)_n^{2n-}$ chains are connected by Na^+–hydrazine–Na^+ bridges, facilitating mutual alignment of the chains along the *c*-axis. Further details on the diffraction data are provided in the Supporting Information, Table S1.

The structure of sodium selenocadmate shares aspects of both neutral low-dimensional metal chalcogenides and anionic chalcogenidometallates. Low-dimensional metal chalcogenides have been synthesized solvothermally from a metal salt and elemental chalcogen, and the resulting structures are one-, two-, or three-dimensional segments of the bulk lattice.[21−23,25,46,47] The extended one-dimensional framework of $Na_2Cd_2Se_3$ is similar to that of the solids $SnS_4Mn_2(N_2H_4)_6$ and ZnTe(1,3-propanediamine) or the hydrazine-soluble species (N_2H_4)-ZnTe.[23,31,47] However, $(Cd_2Se_3)_n^{2n-}$ deviates from the bulk structure of corner-sharing $[CdSe_4]$ tetrahedra and demonstrates the bonding motif of edge-sharing tetrahedra. Edge-sharing brings the cations into closer proximity, yielding a Cd–Cd distance of ~3.34 Å in $Na_2Cd_2Se_3$ compared to a Cd–Cd distance of 4.3 Å in wurtzite CdSe. This suggests greater covalent character that limits the repulsion of the Cd cationic centers. The divergence from bulk structure in favor of edge-sharing tetrahedra is seen in many small molecular chalcogenidometallates (e.g., $Sn_2S_6^{4-}$, $Sn_2Se_6^{4-}$, and $Ge_2Se_6^{4-}$)[28,30] and is exhibited by the extended one-dimensional tellurocadmate polyanion $(CdTe_2)_n^{2n-}$.[36]

The toxicity and instability of hydrazine make the use of other solvents desirable for solution processing; however, sodium selenocadmate has not been appreciably soluble in other solvents tested (DMF, NMF, FA, DMSO, and en). We found that the solubility and versatility of selenocadmate can be expanded by exchanging the charge-balancing cation as schematically shown in Figure 2a. Sodium ions can be replaced

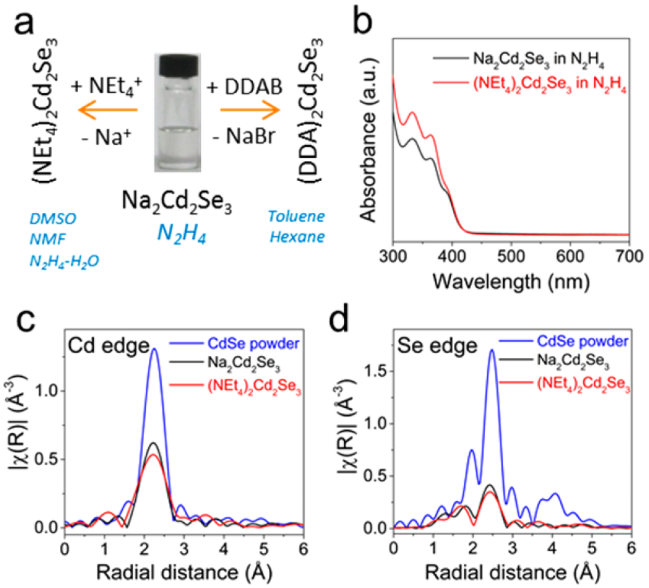

Figure 2. (a) Cation exchange enables solubility of $Na_2Cd_2Se_3$ in various polar and nonpolar solvents. (b) UV–vis absorption spectra suggest that cation exchange does not change the anion. EXAFS data from the (c) Cd and (d) Se K-edges demonstrate the reduced coordination number and increased disorder for $Na_2Cd_2Se_3$ and $(NEt_4)_2Cd_2Se_3$ species in solution.

with tetraethylammonium by stirring a $Na_2Cd_2Se_3$ solution with an excess of NEt_4^+-loaded Amberlyst-15 cation-exchange resin, and the resulting $(NEt_4)_2Cd_2Se_3$ is soluble in hydrazine, 85:15 acetonitrile/hydrazine, *N*-methylformamide, and dimethyl sulfoxide. The solubility can be further expanded to nonpolar solvents by replacing sodium with didodecyldimethylammonium (DDA^+). This cation exchange takes place in a two-phase system where solutions of didodecyldimethylammonium bromide (DDAB) in toluene or hexane and $Na_2Cd_2Se_3$ in hydrazine are stirred, and the selenocadmate transfers to the nonpolar phase. UV–vis spectra for cation-exchanged selenocadmate in a variety of polar and nonpolar solvents are given in the Supporting Information (Figure S2).

The solution structure of the selenocadmate species in hydrazine was further evaluated with extended X-ray absorption fine structure (EXAFS) at the Cd and Se K-edges. The details of a first-shell fit for CdSe powder and $Na_2Cd_2Se_3$ and

DOI: 10.1021/jacs.6b10077
J. Am. Chem. Soc. 2017, 139, 3368−3377

$(NEt_4)_2Cd_2Se_3$ solutions in hydrazine at the Cd and Se edges are given in the Supporting Information (Table S2 and Figures S3–S5). The plots of the Fourier-transformed absorption probability suggest that the selenocadmate structure differs significantly from that of bulk CdSe but does not change dramatically with cation exchange (Figure 2c,d). The reduced amplitude of the Fourier-transformed X-ray absorption for selenocadmate compared to that of bulk CdSe suggests that these species have fewer nearest neighbor contacts between Cd and Se, though the similar shape of the curves indicates that the distance between Cd and Se in selenocadmate is consistent with bulk bond lengths. The coordination numbers for Cd and Se based on the crystal structure of solid $Na_2Cd_2Se_3$ are higher than those predicted by fitting EXAFS data; this suggests that in solution the selenocadmate ions exist as smaller fragments that reorganize into long chains as hydrazine is removed. The signal-to-noise ratio of the EXAFS signal was limited by the low solubility of selenocadmate, complicating further quantitative analysis of the EXAFS fits.

The electronic structure of selenocadmate in solution was explored with UV–vis absorption spectroscopy. Both sodium and tetraethylammonium selenocadmate in hydrazine show similar absorption spectra with peaks at 332 and 363 nm and a shoulder around 390 nm (Figure 2b). The close similarity of the spectra indicates that changing the cation does not significantly change the electronic properties of the selenocadmate anion. Interestingly, the absorption frequencies in these spectra are similar to those seen for CdSe clusters.[48−51] However, a comparison of EXAFS data for sodium selenocadmate and CdSe clusters clearly demonstrates that they are distinct species (Figure S6). This suggests that the UV absorption peaks may correspond to localized excitations of Cd–Se bonds and may be generic to all molecular CdSe species.

3.2. Molecular Selenocadmates as Capping Ligands for Colloidal Nanomaterials. In previous studies we have shown that chalcogenidometallates can be effective capping ligands for colloidal nanoparticles.[36,52] When a solution of $Na_2Cd_2Se_3$ in hydrazine is added to a solution of CdSe nanoparticles capped with *n*-octadecylphosphonate (ODPA) ligands in toluene, the nanoparticle ligands exchange from ODPA to $(Cd_2Se_3)_n^{2n-}$, and the nanoparticles transfer to the hydrazine phase (Figure 3a). Washing the hydrazine with excess toluene removes organics and yields a solution of inorganic-capped CdSe. Transmission electron microscope images (Figure 3b) show that the CdSe nanoparticles retain their morphology upon ligand exchange, and infrared (IR) spectroscopy indicates that the organic ligands are completely removed (Figure 3c). Solutions of $Cd_2Se_3^{2-}$-capped CdSe in hydrazine can be spin-coated onto substrates and annealed at 300 °C to form large grains of polycrystalline CdSe, and field-effect transistors constructed from these films yield electron mobilities of ~300 $cm^2\ V^{-1}\ s^{-1}$.[36,37] This remarkable electron mobility suggests that the composition-matched ligands not only foster semiconductor grain growth during annealing but also improve electronic transport across the grain boundaries, serving as a solder that retains semiconductor performance.

As described above, the use of hydrazine as a solvent limits the conditions under which the solution can be used. We found that performing ligand exchange with $(NEt_4)_2Cd_2Se_3$ rather than $Na_2Cd_2Se_3$ yields $Cd_2Se_3^{2-}$-capped nanoparticles that can be dissolved in the more benign solvent *N*-methylformamide (NMF). Ligand exchange was performed as described above

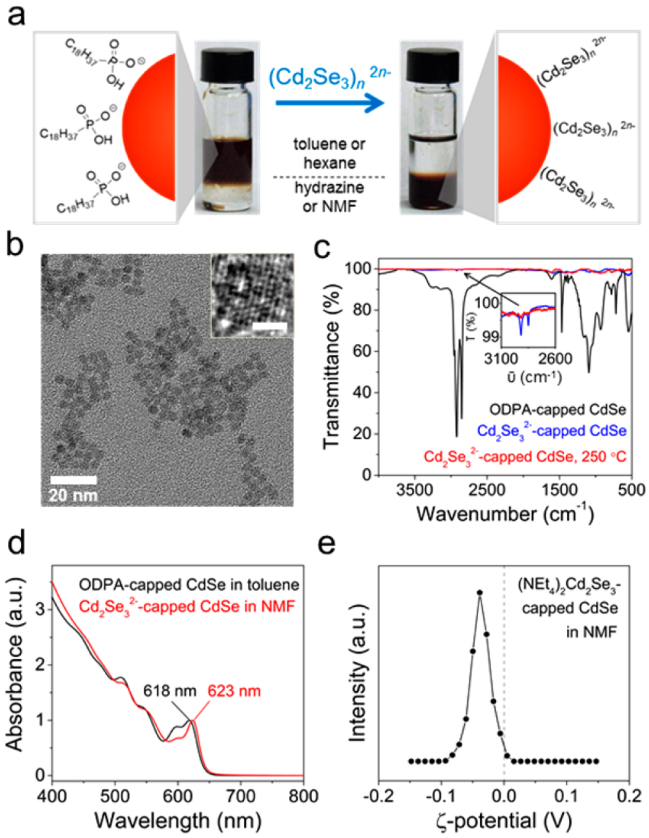

Figure 3. (a) Schematic showing the ligand exchange of CdSe nanoparticles from ODPA to $(Cd_2Se_3)_n^{2n-}$ and the corresponding phase transfer. (b) TEM image of $Na_2Cd_2Se_3$-capped CdSe nanoparticles with an inset showing lattice fringes, scale bar 2 nm. (c) IR shows that signals corresponding to organic ligands are gone after ligand exchange with $Na_2Cd_2Se_3$. (d) UV–vis of solutions of ODPA-capped CdSe in toluene and $(NEt_4)_2Cd_2Se_3$-capped CdSe in NMF. (e) Zeta potential measurement of $(NEt_4)_2Cd_2Se_3$-capped CdSe in NMF with the peak centered at approximately −40 mV.

with a solution of $(NEt_4)_2Cd_2Se_3$ in hydrazine. The ligand-exchanged nanoparticles could be precipitated with an excess of acetonitrile and dissolved in NMF. UV–vis measurements of solutions of CdSe nanoparticles before and after ligand exchange indicate that the nanoparticles have retained their size and were transferred into the polar solvent. The zeta potential of the $Cd_2Se_3^{2-}$-capped CdSe in NMF was approximately −40 mV, suggesting that $(Cd_2Se_3)_n^{2n-}$ is bound to the nanocrystals and stabilizes the nanocrystals in solution via charge repulsion. Comparable zeta potentials have been measured for many chalcogenidometallate-capped nanoparticles.[52]

3.3. Templated Synthesis of Mesostructured II–VI Semiconductors. The facile interchange of charge-balancing cations in solution allows for templating of chalcogenidocadmate ions using long-chain alkylammonium surfactants to form unprecedented mesoporous CdSe and CdTe structures (Figure 4a). Organic surfactants have been previously used as a soft template for inorganic materials to produce solids with monodisperse mesoscale (2–50 nm) pores in an organized array.[53] Surfactant-templated mesoporous oxides have been widely utilized for their high surface area and the ease of surface functionalization. Functionalized mesoporous oxides display high performance in many applications, including heteroge-

DOI: 10.1021/jacs.6b10077
J. Am. Chem. Soc. 2017, 139, 3368–3377

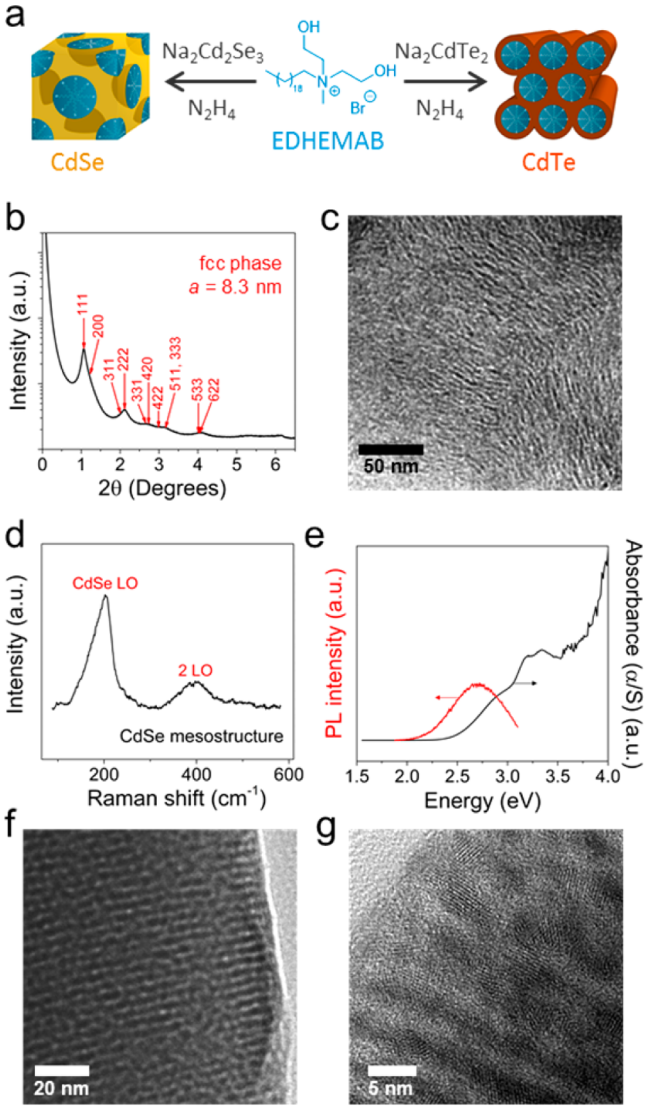

Figure 4. (a) Proposed scheme depicting the soft templating of chalcogenidocadmates. Characterization of mesostructured (b–e) CdSe and (f, g) CdTe. (b) The SAXS pattern for mesostructured CdSe shows long-range order that can be indexed to an fcc lattice. TEM images of mesostructured (c) CdSe and (f, g) CdTe show clear areas of metal chalcogenide separated by surfactant-filled pores. (d) The Raman spectrum for the CdSe mesostructure shows broad peaks corresponding to CdSe. (e) The diffuse reflectance (converted to absorbance with Kubleka–Munk equation) and photoluminescence of a mesostructured CdSe film excited at 3.26 eV indicate a bandgap of ~2.5 eV.

neous catalysts, solar cell absorber layers, and cathode and anode materials for Li ion batteries.[53−55] It is hoped that the extension of soft templating techniques to non-oxide II–VI semiconductors will yield novel functional materials. Previous reports have demonstrated the patterning of chalcogenidometallates (e.g., $Sn_2S_6^{4-}$, $SnTe_4^{4-}$, and $Ge_4S_{10}^{4-}$) around columnar micelles and cross-linking of the resulting structure with transition metal ions (Pt^{2+}, Pt^{4+}, Cd^{2+}, Zn^{2+}, or Mn^{2+}).[39,40,56] These reports suggest that the oligomerization of chalcogenidometallate species through interaction with metal ions is necessary for the mesostructure formation to be entropically allowed; however, the extended chains of $(Cd_2Se_3)_n^{2n-}$ or $(CdTe_2)_n^{2n-}$ favorably self-assemble with positively charged micelles without the inclusion of a foreign metal ion. This work is to our knowledge the first example of surfactant-templated CdSe and CdTe from molecular precursors.

An ordered CdSe mesostructure can be formed by coprecipitation of *N*-eicosane-*N*,*N*-di(2-hydroxyethyl)-*N*-methylammonium bromide (EDHEMAB) and $(Cd_2Se_3)_n^{2n-}$ from hydrazine. When a colorless solution of $Na_2Cd_2Se_3$ in hydrazine is added to EDHEMAB solution in hydrazine at 80 °C, the resulting mixture immediately turns a cloudy white. After stirring the reaction mixture for 3 h at 40 °C, the precipitate is collected by centrifugation and washed with excess ethanol and hexane to yield a yellow powder.

The organization of the resulting hybrid inorganic–organic mesostructure was explored with SAXS and transmission electron microscopy (TEM). Small-angle X-ray scattering (SAXS) at the Advanced Photon Source at Argonne National Lab was used to probe the mesoscale order of a large powder sample without selection bias. The SAXS pattern shows a number of resolved peaks and indicates a mesostructure with long-range order of the pores (Figure 4b). These peaks can be indexed to a face-centered cubic lattice of spherical surfactant micelles surrounded by metal chalcogenide, with a possible structure suggested in Figure 4a. Although hexagonal phases of columnar micelles are most often achieved with surfactant templating, the formation of cubic phases has been seen for both metal oxides[57] and chalcogenides,[40,56] and it has been suggested that cubic phases are more desirable because guest species can access the porous network from all directions. It is possible that the relatively low reaction temperature or the reaction of selenocadmate with the surfactant and resulting reduction of templating species yields spherical rather than columnar micelles.

Transmission electron microscopy was used to further explore the morphology of this mesostructured CdSe. TEM images show large areas of mesostructure with surfactant-filled pores of about 2 nm diameter (Figure 4c and Figure S7). However, the TEM images do not reflect the long-range order suggested by SAXS measurements but rather suggest disordered, wormhole-like pores. This discrepancy is likely due to the difference in sample preparation for the two techniques. SAXS measurements were taken on a wet powder suspended in ethanol, while TEM measurements were taken on a dry powder under high vacuum. The change of mesostructure organization upon drying is a known phenomenon and is here demonstrated by our two techniques.[58,59] It is likely that ethanol swells the organic template, and order is lost as the template dries and contracts.

ICP-OES of the mesostructured CdSe powder indicates that the material contains equimolar amounts of Cd and Se (Table S3). The excess selenium in the $Na_2Cd_2Se_3$ precursor likely reacts with the surfactant to yield CdSe and volatile or soluble byproducts that are removed during washing. The dealkylation of alkylammonium salts by chalcogenides is well-known and could easily occur at the elevated temperature of the template solution to release a soluble organoselenium species.[58] Although ICP-OES indicates stoichiometric CdSe, powder X-ray diffraction (XRD) shows only broad peaks at higher angles (Figure S8), suggesting that the pore walls are either amorphous or contain very small crystallites. The Raman spectrum of mesoporous powder exhibits peaks at ~202 and ~404 cm^{-1} corresponding to the longitudinal optical (LO) phonon mode of CdSe lattice and its first overtone (Figure 4d). For comparison, the Raman spectrum of $Na_2Cd_2Se_3$ is

DOI: 10.1021/jacs.6b10077
J. Am. Chem. Soc. 2017, 139, 3368–3377

qualitatively different from that of CdSe (Figure S9), further confirming that the mesostructured material contains a CdSe phase formed from templated $(Cd_2Se_3)_n^{2n-}$ ions under our reaction conditions. Thermogravimetric analysis indicates that the pores are filled with surfactant which is removed at elevated temperature (Figure S10). The diffuse reflectance spectrum of a film of mesostructured CdSe was measured with an integrating sphere and converted to absorbance using the Kubelka–Munk equation (Figure 4e and Figure S11). This measurement indicates a bandgap of ~2.5 eV, which is reasonable for strongly quantum-confined CdSe.[9] The photoluminescence of a film of mesostructured CdSe excited at 3.26 eV was measured, and it agrees with the bandgap measured by diffuse reflectance (Figure 4e).

This technique for creating surfactant-templated metal chalcogenides can be extended to form mesostructured CdTe. When solutions of Na_2CdTe_2 in hydrazine and EDHEMAB in formamide are combined at 80 °C, a yellow-orange precipitate forms immediately, and the solution turns green due to decomposition of tellurocadmate to yield polytelluride and CdTe. The resulting suspension is stirred at room temperature for an hour, and a deep red-orange powder is isolated by centrifugation and washed with ethanol and hexane to remove the excess surfactant and tellurium. TEM reveals a well-ordered CdTe mesostructure templated around columnar micelles (Figure 4f). Though XRD shows no sharp peaks at high 2θ angles (Figure S11a), the identity of the metal chalcogenide was confirmed with Raman spectroscopy (Figure S11b). The lattice fringes of small crystallites can be seen in the high-resolution TEM image (Figure 4g), likely due to crystallization of amorphous CdTe under the electron beam. A natural follow-up to these syntheses is the removal of the templating surfactant or the use of a semiconducting templating agent to create new functional materials.[59]

3.4. Gel-like Stoichiometric CdSe·xN_2H_4. Unlike the facile replacement of Na^+ by organic cations, the addition of Cd^{2+} to $(Cd_2Se_3)_n^{2n-}$ induces significant changes in the chalcogenidometallate structure and properties, creating a novel gel-like form of CdSe. When $Na_2Cd_2Se_3$ is combined with $CdCl_2$ in hydrazine, an off-white suspension forms (Figure 5a), based on the following equation:

$$Na_2Cd_2Se_3 + CdCl_2 \xrightarrow{N_2H_4} 3CdSe{\cdot}xN_2H_4(gel) + 2NaCl \quad (1)$$

Brief centrifugation yields a viscous gel-like material, and the soluble NaCl product is removed in the supernatant. ICP-OES confirms that this gel-like species contains equimolar amounts of Cd and Se and negligible Na. This CdSe gel is related to a class of chalcogels created by cross-linking chalcogenidometallates (e.g., $[Sn_2S_6]^{4-}$ and $[Ge_4S_{10}]^{4-}$) with transition metal ions; however, chalcogels typically use foreign metal ions (e.g., Pt^{2+}) to control the cross-linking metathesis and produce a stable gel.[60,61] Stoichiometric CdSe gel is attractive as a precursor for semiconductor materials because its only possible contaminant is hydrazine, which readily evaporates during annealing to leave a chemically pure CdSe phase, and its high viscosity is convenient for doctor blading and other deposition techniques.

Raman spectroscopy, powder X-ray diffraction, and EXAFS were used to examine the structure of CdSe gel. The Raman spectrum of CdSe gel displays a peak at 140 cm^{-1} and a broad feature below 250 cm^{-1} (Figure 5b); these features are distinct from those of both bulk CdSe and $Na_2Cd_2Se_3$ (Figure S9),

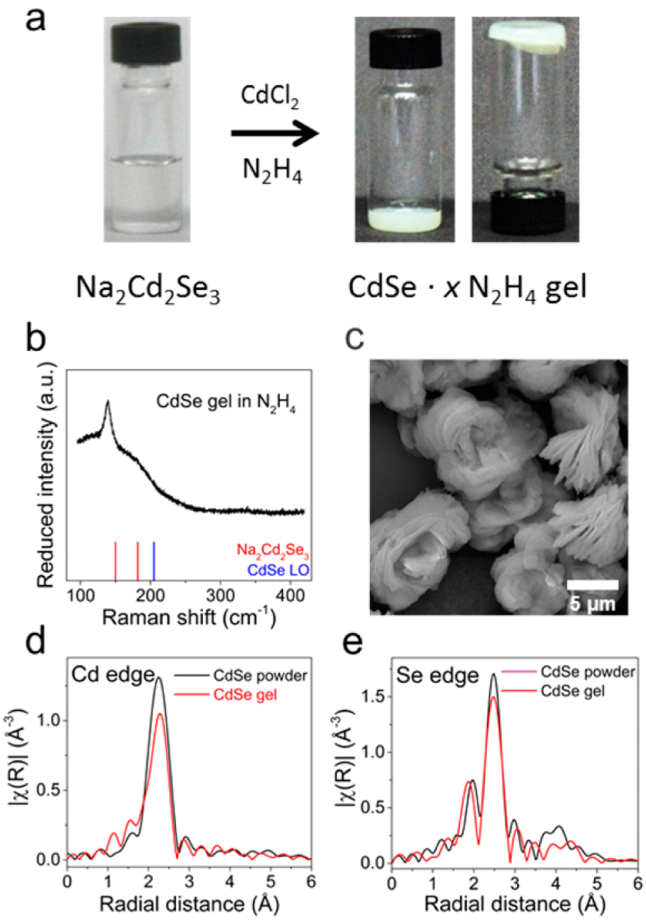

Figure 5. (a) Photographs showing the synthesis of CdSe gel and its high viscosity. (b) The Raman spectrum of CdSe gel has a sharp feature at 140 cm^{-1}, which does not correspond to the features of $Na_2Cd_2Se_3$ or CdSe. (c) The SEM image of dried CdSe gel has aggregations of thin sheets. EXAFS data from the (d) Cd and (e) Se K-edges suggests that the CdSe gel has a structure similar to that of bulk CdSe.

indicating different chemical bonding in these compounds. The appearance of peaks below the energy of the phonon modes of the parent compound has been observed for low-dimensional metal chalcogenides,[47] suggesting that the CdSe gel may have isolated fragments of a tetrahedrally coordinated CdSe lattice.

The structure of this stoichiometric CdSe gel was explored with powder XRD. Removal of the hydrazine solvent leads to structural collapse of the gel material, yielding a yellow to orange powder that cannot be resuspended in hydrazine, so XRD measurements were taken on suspensions of the gel in hydrazine held in sealed glass capillaries. The suspension is largely amorphous and exhibits only weak scattering; however, rings can be observed in the two-dimensional powder patterns (Figures S13 and S14). Immediately after synthesis, the diffraction pattern exhibits one peak at ~8° 2θ angle, but the structure evolves over time, developing peaks at higher angles as the initial peak wanes in intensity. The structure stabilizes after 24 h, exhibiting two diffraction peaks at ~10.5° and ~27° 2θ, and this structure remains stable in a sealed nitrogen atmosphere (no observed changes up to 60 days).

The poor crystallinity of the CdSe gel limits the quality of attainable powder data, so direct structure solution followed by Rietveld refinement is not possible. However, we noted that the peak positions and intensities are similar to those previously

DOI: 10.1021/jacs.6b10077
J. Am. Chem. Soc. 2017, 139, 3368–3377

seen for layered metal chalcogenides with bridging diamines. Powder XRD patterns for CdS, CdSe, and CdTe layered structures with linking amines have the most intense peak at a low angle; 10.6° 2θ is reported for layered CdSe slabs linked by ethylenediamine[21] and 8.6° 2θ is reported for CdSe slabs linked by 1,3-propanediamine.[47] These intense peaks correspond to the interslab spacing, with larger distances yielding diffraction at smaller angles. Thus, the observed peaks in CdSe gel at low angles may suggest that layered slabs of a 2-dimensional CdSe species have formed. The evolution of the diffraction peaks with time may represent the formation of different layered CdSe structures with variable distance between slabs; we expect that hydrazine fills the space between layers and is expelled as the structure evolves as schematically outlined in Scheme S1. The SEM images of dried gel show micron-sized globules with an internal structure made of stacked layers (Figure 5c), supporting the above hypothesis. Additionally, thermogravimetric analysis suggests that the gel composition is approximately $4CdSe{\cdot}3N_2H_4$; two loosely bound hydrazine molecules are lost at ~100 °C, and a chemically bound hydrazine is lost at ~200 °C to yield pure CdSe (Figure S16). Further analysis of the gel structure is provided in the Supporting Information (Figures S14 and S15, Table S4).

EXAFS measurements taken on the CdSe gel suspension in hydrazine further support the proposed structure model. The amplitude of the Fourier-transformed absorption probability of the gel is higher than that of selenocadmate and more closely mimics bulk CdSe, suggesting higher coordination numbers for Cd and Se (Figure 5d,e). Fitting of this data (Table S2) yields coordination numbers of about 3.5 ± 0.6 for both Cd and Se. The chains of $(Cd_2Se_3)_n^{2n-}$ have cross-linked through addition of Cd^{2+}, creating many new Cd−Se bonds and a structure that approaches that of bulk CdSe. Additionally, the Cd edge is well-modeled with the inclusion of a nitrogen shell, suggesting that cadmium is directly coordinated to hydrazine. It is likely that the edges of the slabs have under-coordinated cadmium that is bound to hydrazine. This direct coordination of amines to cadmium has been shown to stabilize a variety of low-dimensional metal chalcogenide species.[21−23] Hydrazine coordination supports the separation of the chains and formation of an open gel structure, and the replacement of these Cd−N bonds with Cd−Se likely leads to the gel collapse and the formation of sphalerite or wurtzite CdSe. Indeed, upon annealing the gel collapses to form a crystalline CdSe phase as shown schematically in Figure 6a.

Suspensions of CdSe gel in hydrazine can be drop-cast onto hydrophilic glass or silicon to form films. Upon annealing, the gel loses coordinated hydrazine and decomposes to wurtzite CdSe; XRD shows that wurtzite CdSe forms as low as 200 °C and grows into larger grains at elevated temperature (Figure 6b). The chemical and phase purity of the obtained CdSe is confirmed by Raman spectroscopy (Figure 6c). SEM of a film annealed at 350 °C reveals that rather than forming a continuous layer, the gel has formed into layered sheets of crystalline CdSe (Figure 6d). Previous works demonstrate that bound amines can template low-dimensional metal chalcogenide precursors to form rod- or sheet-like crystals,[21,22] and the bound hydrazine in the CdSe gel likely induces the formation of sheet-like crystals rather than three-dimensional grains. The porous nature of this film may allow for the intercalation of a second material to create composite materials.

The photoconductivity of an annealed gel film was measured to determine the electronic performance of the material. Figure

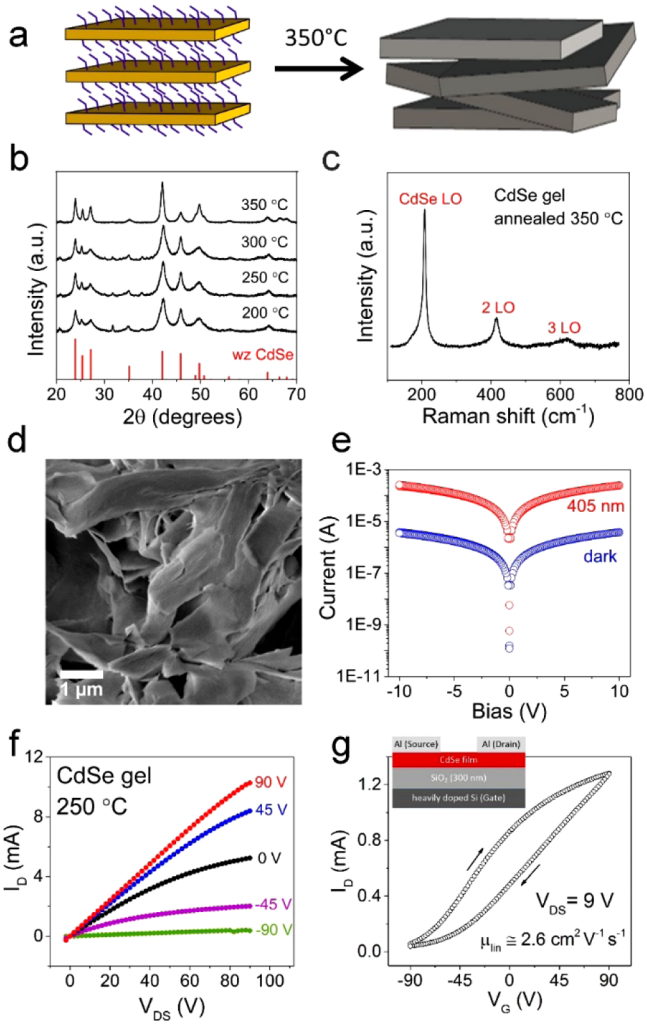

Figure 6. (a) Schematic demonstrating the collapse of the layered gel precursor upon annealing to form sheet-like crystals of CdSe. (b) XRD of CdSe gel films annealed at various temperatures for 30 min under nitrogen with reference peaks shown for wurtzite CdSe. (c) Raman spectrum of annealed CdSe gel shows peaks characteristic of bulk CdSe. (d) SEM image of CdSe gel annealed at 350 °C displays sheet-like grains of CdSe. (e) Photoconductivity of an unwashed CdSe gel film annealed at 350 °C for 30 min. (f) Output and (g) transfer characteristics for an FET with a channel made of an annealed CdSe gel layer. Inset shows a scheme of the FET device used for the measurements. Aluminum contacts (100 nm thick) were thermally evaporated onto the film through a shadow mask (channel length, 50 μm; channel width, 1500 μm).

6e and Figure S16 show the enhanced photocurrent through the gel film when illuminated with a 405 nm laser. The ~60-fold increase in conductivity upon illumination suggests that the CdSe gel film is not degenerately doped. Moreover, the measured conductivity across a large channel (~2 mm) suggests that there is a continuous path for electrons, although the film consists of two-dimensional sheets (Figure 6d).

Further electronic characterization was performed by measuring a field-effect transistor (FET) with an annealed CdSe gel channel. The as-synthesized CdSe gel could not be used to make FETs because the drop-cast film is too thick to effectively gate, and the gel does not form a uniform layer when spin-coated. Instead, we spin-coated a thin layer of $Na_2Cd_2Se_3$ onto a heavily doped silicon substrate with a 300 nm SiO_2 gate

DOI: 10.1021/jacs.6b10077
J. Am. Chem. Soc. 2017, 139, 3368−3377

layer and soaked the resulting film in a $CdCl_2$ solution in methanol. We thus formed a thin layer of CdSe gel on the substrate and annealed the film at 250 °C for 30 min to form polycrystalline CdSe. The electron mobility of the annealed gel film was measured with a standard top-contact bottom-gate FET geometry (Scheme S2). The output and transfer characteristics (Figure 6f,g) indicate a clear gating effect with n-type operation and an extracted linear range electron mobility of 2.6 $cm^2\ V^{-1}\ s^{-1}$. The large negative bias required to deplete the channel indicates n-type doping in the FET channel. Similar FET measurements for gel films annealed at higher temperature show increased off-currents and a further increase in the zero-gate electron concentration in the channel (Figure S18). To explore the origin of n-type doping, we fabricated FETs with channels made of hydrazinium selenocadmate that were not treated with the gel-forming $CdCl_2$ solution and thus not containing Cl^-. The FET transfer curves showed a substantially lower n-type doping level resulting in FET threshold voltages, V_{th}, shifted from about −60 V (FET operates in the depletion mode) in devices made of CdSe gel to about +40 V (FET operates in the accumulation mode) in devices made of hydrazinium selenocadmate (Figure S19). Thus, the room-temperature cross-linking of selenocadmate by $CdCl_2$ seems to affect transport in annealed films primarily by altering the doping level, presumably by thermally activated diffusion of Cl^- ions to substitutional lattice sites where they act as the donor species. The use of other Cd(II) salts may provide a convenient way to control the doping level and carrier mobility in II−VI materials prepared from the gel precursors.

The values of electron mobility measured for FETs with channels made of annealed CdSe gel are comparable to many other nanocrystalline solution-deposited semiconductors,[28,62−64] but considerably lower than the mobilities observed for the spin-coated layers of nanoparticles linked with selenocadmate ligands.[36,37] This difference can be explained by the fact that the field-effect mobility depends primarily on the quality of the interface between the semiconductor channel and the gate dielectric. Since all charge transport occurs within an accumulation layer only a few nanometers thick, high-mobility FETs use thin continuous semiconductor layers; however, the morphology of our "fluffy" CdSe gel is not optimal for high FET mobility. Instead, the open-framework CdSe chains, gels, and mesoporous structures are naturally suitable for building nanoscale composites, soldering semiconductor grains, and utilizing inorganic semiconductors in other unprecedented ways.

4. CONCLUDING REMARKS

We have demonstrated the synthesis and structure of sodium selenocadmate and its modification through interaction with various cationic species to yield new forms of II−VI materials. The one-dimensional selenocadmate polyanion serves as a link between small molecule metal chalcogenide complexes and extended structures, such as nanocrystals[9] and organic−inorganic hybrids synthesized with solid-state or solvothermal syntheses.[21−23] The unique balance of reactivity and stabilization afforded by the hydrazine solvent aids in the creation of an infinite one-dimensional species that retains solubility.

The coordination chemistry of hydrazine is rich, unusual, and underexplored. In many respects, N_2H_4 is an easier-to-handle form of liquid ammonia, showing a strong ability to coordinate and solubilize molecular species. N_2H_4 can be also related to another important ligand, 1,2-ethylenediamine (en), and its derivatives. However, en typically generates chelated complexes, while chelating a metal center with N_2H_4 would require formation of a strained 3-membered ring and is therefore highly unlikely. Instead, the two lone pairs prefer to form a bridge between two metal centers, thus favoring the formation of unprecedented coordination frameworks. In combination with the rich redox chemistry (N_2H_4 is mostly known as a reducing agent but can also behave as an oxidant), we have a powerful agent for the synthesis of low-dimensional semiconductors.[35] Another important benefit of N_2H_4 is its ability to cleanly decompose at relatively low temperatures without leaving behind any carbon-containing impurities.

The synthesis of mesoporous materials by templating inorganic species around organic templates is well-developed for oxides. However, the creation of templated II−VI semiconductors is much less explored and often suffers from the inclusion of impurities, such as foreign metal cations or other linking agents. We have presented a method to form mesostructured CdSe or CdTe using a surfactant template for one-dimensional chalcogenidocadmate polyanions. The polymeric nature of the chalcogenidocadmates allows for favorable coassembly in the presence of a surfactant solution. Further development of these materials could yield mesoporous II−VI materials with inherent optical and electronic properties that cannot be realized in unfunctionalized oxide materials. Finally, the gel-like materials described in this work represent a novel type of precursors for stoichiometric CdSe. This route appears to be particularly useful for semiconducting materials, which demand high chemical purity and structural perfection.

The chemistry presented in this work is not limited to CdSe but can be extended to other semiconductors in the II−VI family. Stable chalcogenidometallates have been previously reported for CdTe,[36,65] ZnTe,[31] HgS,[66] HgSe,[67] and HgTe.[65] Our study suggests that cations play an important role in determining solubility of chalcogenidometallates in polar and nonpolar solvents. We expect that the techniques demonstrated here for CdSe could be extended to other systems with the aid of this prior art. The mixing and matching of semiconducting components at the nanoscale represents a powerful strategy toward materials with advanced physical and chemical properties.

■ ASSOCIATED CONTENT

Supporting Information

The Supporting Information is available free of charge on the ACS Publications website at DOI: 10.1021/jacs.6b10077.

Experimental details and supporting figures (PDF)

■ AUTHOR INFORMATION

Corresponding Author

*dvtalapin@uchicago.edu

ORCID

Margaret H. Hudson: 0000-0002-8977-8139

Byeongdu Lee: 0000-0003-2514-8805

Dmitri V. Talapin: 0000-0002-6414-8587

Present Address

[‖]Department of Energy Engineering, Hanyang University, Seoul 133-791, Republic of Korea.

Notes

The authors declare no competing financial interest.

DOI: 10.1021/jacs.6b10077
J. Am. Chem. Soc. 2017, 139, 3368−3377

■ ACKNOWLEDGMENTS

The authors thank Danny Haubold for assistance with TEM and Michael A. Boles for help with editing. This work was supported by the NSF under Awards CHE-1611331 and DMR-1629601, the Department of Defense (DOD) Air Force Office of Scientific Research under Grant FA9550-14-1-0367, and by the II−VI Foundation. B.L. and D. V. T. were supported by MICCoM as part of the Computational Materials Sciences Program funded by the U.S. Department of Energy, Office of Science, Basic Energy Sciences, Materials Sciences and Engineering Division. Sector 20 facilities at the Advanced Photon Source, and research at these facilities, are supported by the US Department of Energy—Basic Energy Sciences, the Canadian Light Source and its funding partners, and the Advanced Photon Source. This work used resources of the Advanced Photon Source and Center for Nanoscale Materials, a U.S. Department of Energy (DOE) Office of Science User Facilities operated for the DOE Office of Science by Argonne National Laboratory under Contract DE-AC02-06CH11357.

■ REFERENCES

(1) Sze, S. M. *Semiconductor Devices: Physics and Technology*; John Wiley and Sons, Inc.: New York, 2002.
(2) Burst, J. M.; Duenow, J. N.; Albin, D. S.; Colegrove, E.; Reese, M. O.; Aguiar, J. A.; Jiang, C. S.; Patel, M. K.; Al-Jassim, M. M.; Kuciauskas, D.; Swain, S.; Ablekim, T.; Lynn, K. G.; Metzger, W. K. *Nat. Energy* **2016**, *1*, 16015.
(3) Zhang, H.; Kurley, J. M.; Russell, J. C.; Jang, J.; Talapin, D. V. *J. Am. Chem. Soc.* **2016**, *138*, 7464−7467.
(4) Amirav, L.; Alivisatos, A. P. *J. Phys. Chem. Lett.* **2010**, *1*, 1051−1054.
(5) Kudo, A.; Miseki, Y. *Chem. Soc. Rev.* **2009**, *38*, 253−278.
(6) Keuleyan, S.; Lhuillier, E.; Brajuskovic, V.; Guyot-Sionnest, P. *Nat. Photonics* **2011**, *5*, 489−493.
(7) Guyot-Sionnest, P.; Roberts, J. A. *Appl. Phys. Lett.* **2015**, *107*, 253104.
(8) Murray, C. B.; Kagan, C. R.; Bawendi, M. G. *Annu. Rev. Mater. Sci.* **2000**, *30*, 545−610.
(9) Murray, C. B.; Norris, D. J.; Bawendi, M. G. *J. Am. Chem. Soc.* **1993**, *115*, 8706−8715.
(10) Peng, X.; Manna, L.; Yang, W.; Wickham, J.; Scher, E.; Kadavanich, A.; Alivisatos, A. P. *Nature* **2000**, *404*, 59−61.
(11) Milliron, D. J.; Hughes, S. M.; Cui, Y.; Manna, L.; Li, J.; Wang, L.-W.; Alivisatos, A. P. *Nature* **2004**, *430*, 190−195.
(12) Talapin, D. V.; Nelson, J. H.; Shevchenko, E. V.; Aloni, S.; Sadtler, B.; Alivisatos, A. P. *Nano Lett.* **2007**, *7*, 2951−2959.
(13) Nasilowski, M.; Mahler, B.; Lhuillier, E.; Ithurria, S.; Dubertret, B. *Chem. Rev.* **2016**, *116*, 10934−10982.
(14) Ithurria, S.; Talapin, D. V. *J. Am. Chem. Soc.* **2012**, *134*, 18585−18590.
(15) Bruchez, J. M.; Moronne, M.; Gin, P.; Weiss, S.; Alivisatos, A. P. *Science* **1998**, *281*, 2013−2016.
(16) Talapin, D. V.; Steckel, J. *MRS Bull.* **2013**, *38*, 685−695.
(17) Klimov, V. I. *Nanocrystal Quantum Dots*, 2nd ed.; CRC Press, 2010; p 485.
(18) Sahu, A.; Kang, M. S.; Kompch, A.; Notthoff, C.; Wills, A. W.; Deng, D.; Winterer, M.; Frisbie, C. D.; Norris, D. J. *Nano Lett.* **2012**, *12*, 2587−2594.
(19) Lee, J. S.; Kovalenko, M. V.; Huang, J.; Chung, D. S.; Talapin, D. V. *Nat. Nanotechnol.* **2011**, *6*, 348−352.
(20) Choi, J. H.; Fafarman, A. T.; Oh, S. J.; Ko, D. K.; Kim, D. K.; Diroll, B. T.; Muramoto, S.; Gillen, J. G.; Murray, C. B.; Kagan, C. R. *Nano Lett.* **2012**, *12*, 2631−2638.
(21) Deng, Z.-X.; Li, L.; Li, Y. *Inorg. Chem.* **2003**, *42*, 2331−2341.
(22) Yao, H.-B.; Gao, M.-R.; Yu, S.-H. *Nanoscale* **2010**, *2*, 323−334.
(23) Yuan, M.; Dirmyer, M.; Badding, J.; Sen, A.; Dahlberg, M.; Schiffer, P. *Inorg. Chem.* **2007**, *46*, 7238−7240.
(24) Bronger, W.; Muller, P. *J. Less-Common Met.* **1984**, *100*, 241−247.
(25) Sheldrick, W. S.; Wachhold, M. *Angew. Chem., Int. Ed. Engl.* **1997**, *36*, 206−224.
(26) Scott, R. W. J.; MacLachlan, M. J.; Ozin, G. A. *Curr. Opin. Solid State Mater. Sci.* **1999**, *4*, 113−121.
(27) Pell, M. A.; Ibers, J. A. *Chem. Ber.* **1997**, *130*, 1−8.
(28) Mitzi, D. B.; Kosbar, L. L.; Murray, C. E.; Copel, M.; Afzali, A. *Nature* **2004**, *428*, 299−303.
(29) Mitzi, D. B.; Copel, M.; Chey, S. J. *Adv. Mater.* **2005**, *17*, 1285−1289.
(30) Mitzi, D. B. *Inorg. Chem.* **2005**, *44*, 3755−3761.
(31) Mitzi, D. B. *Inorg. Chem.* **2005**, *44*, 7078−7086.
(32) Mitzi, D. B.; Copel, M.; Murray, C. E. *Adv. Mater.* **2006**, *18*, 2448−2452.
(33) Mitzi, D. B.; Yuan, M.; Liu, W.; Kellock, A. J.; Chey, S. J.; Deline, V.; Schrott, A. G. *Adv. Mater.* **2008**, *20*, 3657−3662.
(34) Yuan, M.; Mitzi, D. B. *Dalton Trans.* **2009**, 6078−6088.
(35) Mitzi, D. B. *Adv. Mater.* **2009**, *21*, 3141−3158.
(36) Dolzhnikov, D. S.; Zhang, H.; Jang, J.; Son, J. S.; Panthani, M. G.; Shibata, T.; Chattopadhyay, S.; Talapin, D. V. *Science* **2015**, *347*, 425−428.
(37) Jang, J.; Dolzhnikov, D. S.; Liu, W.; Nam, S.; Shim, M.; Talapin, D. V. *Nano Lett.* **2015**, *15*, 6309−6317.
(38) Armatas, G. S.; Kanatzidis, M. G. *Nature* **2006**, *441*, 1122−1125.
(39) Rangan, K. K.; Trikalitis, P. N.; Canlas, C.; Bakas, T.; Weliky, D. P.; Kanatzidis, M. G. *Nano Lett.* **2002**, *2*, 513−517.
(40) Trikalitis, P. N.; Rangan, K. K.; Bakas, T.; Kanatzidis, M. G. *Nature* **2001**, *410*, 671−675.
(41) MacLachlan, M. J.; Coombs, N.; Ozin, G. A. *Nature* **1999**, *397*, 681−684.
(42) Sun, D.; Riley, A. E.; Cadby, A. J.; Richman, E. K.; Korlann, S. D.; Tolbert, S. H. *Nature* **2006**, *441*, 1126−1130.
(43) See Supporting Information for details.
(44) Carbone, L.; Nobile, C.; De Giorgi, M.; Sala, F. D.; Morello, G.; Pompa, P.; Hytch, M.; Snoeck, E.; Fiore, A.; Franchini, I. R.; Nadasan, M.; Silvestre, A. F.; Chiodo, L.; Kudera, S.; Cingolani, R.; Krahne, R.; Manna, L. *Nano Lett.* **2007**, *7*, 2942−2950.
(45) Broxton, T. J.; Chung, R. P. T. *J. Org. Chem.* **1990**, *55*, 3886−3890.
(46) Huang, X.; Li, J. *J. Am. Chem. Soc.* **2007**, *129*, 3157−3162.
(47) Huang, X. Y.; Li, J.; Zhang, Y.; Mascarenhas, A. *J. Am. Chem. Soc.* **2003**, *125*, 7049−7055.
(48) Beecher, A. N.; Yang, X. H.; Palmer, J. H.; LaGrassa, A. L.; Juhas, P.; Billinge, S. J. L.; Owen, J. S. *J. Am. Chem. Soc.* **2014**, *136*, 10645−10653.
(49) Wang, Y. Y.; Liu, Y. H.; Zhang, Y.; Kowalski, P. J.; Rohrs, H. W.; Buhro, W. E. *Inorg. Chem.* **2013**, *52*, 2933−2938.
(50) Evans, C. M.; Love, A. M.; Weiss, E. A. *J. Am. Chem. Soc.* **2012**, *134*, 17298−17305.
(51) Cossairt, B. M.; Owen, J. S. *Chem. Mater.* **2011**, *23*, 3114−3119.
(52) Kovalenko, M. V.; Scheele, M.; Talapin, D. V. *Science* **2009**, *324*, 1417−1420.
(53) Li, W.; Liu, J.; Zhao, D. Y. *Nat. Rev. Mater.* **2016**, *1*, 16023.
(54) Bach, U.; Lupo, D.; Comte, P.; Moser, J. E.; Weissortel, F.; Salbeck, J.; Spreitzer, H.; Gratzel, M. *Nature* **1998**, *395*, 583−585.
(55) Maschmeyer, T.; Rey, F.; Sankar, G.; Thomas, J. M. *Nature* **1995**, *378*, 159−162.
(56) Armatas, G. S.; Kanatzidis, M. G. *Nat. Mater.* **2009**, *8*, 217−222.
(57) Schumacher, K.; Ravikovitch, P. I.; Du Chesne, A.; Neimark, A. V.; Unger, K. K. *Langmuir* **2000**, *16*, 4648−4654.
(58) Ogura, M.; Miyoshi, H.; Naik, S. P.; Okubo, T. *J. Am. Chem. Soc.* **2004**, *126*, 10937−10944.
(59) Chatterjee, P.; Hazra, S.; Amenitsch, H. *Soft Matter* **2012**, *8*, 2956−2964.
(60) Bag, S.; Kanatzidis, M. G. *J. Am. Chem. Soc.* **2010**, *132*, 14951−14959.

DOI: 10.1021/jacs.6b10077
J. Am. Chem. Soc. 2017, 139, 3368−3377

(61) Bag, S.; Trikalitis, P. N.; Chupas, P. J.; Armatas, G. S.; Kanatzidis, M. G. *Science* **2007**, *317*, 490−493.
(62) Ridley, B. A.; Nivi, B.; Jacobson, J. M. *Science* **1999**, *286*, 746−749.
(63) Kagan, C. R.; Mitzi, D. B.; Dimitrakopoulos, C. D. *Science* **1999**, *286*, 945−947.
(64) Kagan, C. R.; Lifshitz, E.; Sargent, E. H.; Talapin, D. V. *Science* **2016**, *353*, aac5523.
(65) Bollinger, J. C.; Roof, L. C.; Smith, D. M.; McConnachie, J. M.; Ibers, J. A. *Inorg. Chem.* **1995**, *34*, 1430−1434.
(66) Sommer, H.; Hoppe, R. *Z. Anorg. Allg. Chem.* **1978**, *443*, 201−211.
(67) Thiele, G.; Lippert, S.; Fahrnbauer, F.; Bron, P.; Oeckler, O.; Rahimi-Iman, A.; Koch, M.; Roling, B.; Dehnen, S. *Chem. Mater.* **2015**, *27*, 4114−4118.

DOI: 10.1021/jacs.6b10077
J. Am. Chem. Soc. 2017, 139, 3368−3377